


Article

Experimental Investigation of the Prestrike Characteristics of a Double-Break Vacuum Circuit Breaker under DC Voltages

Yun Geng¹, Xiaofei Yao^{1,*}, Jinlong Dong^{1,*} , Xue Liu¹, Yingsan Geng¹, Zhiyuan Liu¹, Jing Peng² and Ke Wang²

¹ State Key Laboratory of Electrical Insulation and Power Equipment, Xi'an Jiaotong University, No.28 Xianning West Road, Xi'an 710049, China; gengcloud@163.com (Y.G.); xuel96723@163.com (X.L.); ysgeng@xjtu.edu.cn (Y.G.); liuzy@xjtu.edu.cn (Z.L.)

² Electric Power Research Institute, Yunnan Power Grid Co. Ltd., No.105 Yunda West Road, Kunming 650217, China; pengjinyunnan@126.com (J.P.); wangkeyunnan@126.com (K.W.)

* Correspondence: yaofx85@mail.xjtu.edu.cn (X.Y.); djl.1989@stu.xjtu.edu.cn (J.D.); Tel.: +86-029-82663773 (J.D.)

Received: 1 May 2020; Accepted: 16 June 2020; Published: 20 June 2020



Abstract: The prestrike phenomenon in vacuum circuit breakers (VCBs) is interesting but complicated. Previous studies mainly focus on the prestrike phenomenon in single-break VCBs. However, experimental work on prestrike characteristics of double-break VCBs cannot be found in literature. This paper aims to experimentally determine the probabilistic characteristics of prestrike gaps in a double-break VCB consisting of two commercial vacuum interrupters (VIs) in series under direct current (DC) voltages. As a benchmark, single-break prestrike gaps were measured by short-circuiting one of the VIs in a double break. The experimental results show that the 50% prestrike gap d_{50} of each VI in a double break, which is calculated with the complementary Weibull distribution, was significantly reduced by 25% to 72.7% compared with that in a single break. Due to the voltage-sharing effect in the double-break VCB, scatters in prestrike gaps of each VI in a double break was smaller than that in a single break. However, without the sharing-voltage effect, d_{50} of the low-voltage side in the double break was 65% higher than that of the same VI in the single break, which could be caused by the asynchronous property of mechanical actuators, the difference of the inherent prestrike characteristics of each VI and the unequal voltage-sharing ratio of VIs.

Keywords: vacuum circuit breaker; double break; prestrike characteristics; vacuum interrupter; prestrike gap

1. Introduction

Vacuum circuit breakers (VCBs) are widely used in medium voltage power systems while SF₆ gas circuit breakers are still the prevailing technology in high- and extra high-voltage networks. However, SF₆ gas has been specified as a strong greenhouse gas since 1997 in the Kyoto Protocol and its emission has been strictly restricted. Therefore, it has been of increasing interest to develop VCBs to higher voltage levels due to their advantages such as being maintenance free, having a long mechanical life, excellent dielectric strength, high interruption capability, and environment-friendly characteristics [1].

The major difficulty of extending the application of VCBs to higher voltage levels arises from the physical disadvantage of a vacuum in terms of the dielectric characteristics, i.e., the non-linear relationship between the dielectric strength and contact gap length [2]. To be precise, the breakdown voltage is nearly linear to the vacuum gap length within about 5 mm [3]. However, for a larger gap, the dielectric strength shows a strong full voltage effect. An appropriate way to develop high voltage

level VCBs is to use the double-or multi-break VCBs consisting of two or more vacuum interrupters (VIs) in series, which takes full advantages of the excellent dielectric strength and high interruption capability of short vacuum gaps [4].

Prestrike in VIs happens when the movable contact is approaching the fixed contact during the current-making operation. Once the electric field strength across the contacts becomes larger than the breakdown strength of the vacuum gap, an electric arc may occur prior to the mechanical touch of the contacts, allowing a high inrush or making currents flow through. The prestrike phenomenon in VCBs can cause electromagnetic transients in electrical systems, which may lead to harmful effects and even damage in electrical devices in the system such as transformers, electrical machines and the circuit breaker itself [5]. The pre-breakdown phenomena in VCBs is complicated. There are mainly two theories about the pre-breakdown in VCBs. One is that field-emission current induces breakdown, the other is that microparticles induce vacuum breakdown [6]. If the field strength at the surface of a clean cathode in a VCB exceeds about 2×10^7 V/m, then field emission currents will be observed [7]. If the field strength exceeds about 1×10^8 V/m, pre-breakdown will occur [8]. Pre-breakdown induced by microparticles mainly occurs at larger gap spacing [9].

Numerous efforts have been made to understand the prestrike phenomenon in vacuum interrupters. Some researchers mainly focused on the melting effect of the prestrike arc on the contacts of the VCB, and this effect would affect the breaking performance of the VCB. To study this, Slade et al. [10,11] undertook a series of experiments to find that as the prestrike gap of the single-break VCB increased, the prestrike arc lasted longer. The prestrike arc could cause the contacts to weld and the damage caused by the welding depended on the arcing time. In order to determine the correlation of the prestrike process and the breaking process of the VCB which mainly was researched in the field of switching capacitor banks, Dullni et al. [12] found that the restrike phenomenon had some correlation with the prestrike process mainly due to the protrusions caused by the prestrike arc on the contacts in the single-break VCB. Körner et al. [13,14] obtained similar but more detailed results to Dullni. They found that the significant development of local protrusions on the contact surface affected both the microstructure and the macrostructure of contact surface during the capacitive making and breaking process. Some researchers focused on the welding force caused by the prestrike arc on the contacts of the VCB. If the value of the inrush current was high enough, the contacts would be melted and become welded. The welding force was a basic value that could reflect the melting degree of the contacts. Kumichev et al. [15] found that there was a correlation between welding forces caused by capacitive prestrike process and the number of non-sustained disruptive discharges (NSDDs). Yu et al. [16,17] found that both the amplitude and the scattering of the prestrike gaps and the welding force were significantly influenced by the contact materials about the capacitive current prestrike in single-break VCB. The damage caused by the prestrike arc was mainly influenced by the value of the prestrike current (5 kA, 10 kA or 20 kA). The material and structure of the contacts could also influence the prestrike arc behavior. Geng et al. [18] found that axial-magnetic field (AMF) contacts can effectively reduce the erosion of the contacts produced by the prestrike arc when the capacitive current is generated because of the diffusing effect produced by the AMF in single-break VCB, and higher inrush current value would cause larger damage on the contacts. Some researchers have undertaken calculations and simulations in order to gain an in depth understanding of the prestrike process. A.A. Razi-Kazemi et al. [19] established a new realistic transient model for prestrike phenomena in single-break VCB. Non-linear movement of the contacts, probabilistic behavior of the breakdown voltage and the non-linear dielectric strength curve of the VCB were fully considered in this model. Other researchers focused on the prestrike process mainly due to the design or application of the VCB. X. Ma et al. [20] undertook experiments to observe the direct current (DC) pre-breakdown and breakdown characteristics of micrometric gaps varying from 25 to 1000 μm . The results showed that the pre-breakdown conduction was dominated by high field-electron emission and could be valuable for the design of vacuum gaps in field emission displays. Kharin et al. [21,22], in a series of papers, undertook calculations and experiments to explore the complexity of closing single-break vacuum

interrupter contacts, in order to make an electrical circuit. Sima et al. [23] found that phase-controlled VCBs can reduce the transient overvoltage and overcurrent compared with ordinary VCBs when they were used to switch 10 kV shunt capacitor banks. However, previous studies mainly focus on the prestrike characteristics of single-break VCBs. At present, experimental investigation of the prestrike characteristics of a double-break VCBs has not been reported so far.

The objective of this paper is to determine experimentally the probabilistic characteristics of prestrike gaps in a double-break VCB under DC voltages. This work can provide very important information on the prestrike arcing process, which is of significant importance for the study of the dielectric performance in VIs. Moreover, a better knowledge of the scatter in prestrike gaps in VIs can be very helpful to improve the control accuracy of phase-controlled switching.

2. Experimental Setup

Figure 1 shows an experimental circuit, including a capacitor bank C_s , a double-break VCB, a capacitive-resistance voltage divider, and an auxiliary electrical circuit. Figure 2 shows a picture of the experimental setup. During the experimental tests, the capacitor bank was initially charged to a certain voltage U_s , which was applied to the double-break VCB as soon as the switchgear SW_{DC} was closed. The VCB was then triggered to close the circuit. During the closing operation, the moving contact was approaching the fixed contact leading to a decrement of the dielectric strength of the vacuum gap between the contacts. When the pre-charged voltage exceeded the breakdown voltage of the vacuum gap, prestriking occurred before the mechanical touch of the contacts.

The double-break VCB under test included two commercial 12 kV vacuum interrupters in series, which were denoted VI_A and VI_B as shown in Figure 1. Cup-type AMF contacts were adopted. The contact material was CuCr30 (30% weight of Cr). The surfaces of the contacts were initially well-conditioned. A capacitive-resistance voltage divider, which can reduce the influence of the stray capacitance to ground, was used to measure the voltage U_m across the VCB during the transient prestrike process. When the first prestrike occurred, a stepdown in the measured voltage waveform of U_m was then captured. Moreover, with the help of an auxiliary circuit, which included a battery and two resistors in series that were connected to the auxiliary contact (SW_{au}) of the VCB, the time instant of the mechanical touch of the contacts in VIs can be detected from the waveform of voltage U_a . The displacement curve of the moving contact, denoted by L_{disp} , was measured by using a high-precision linear displacement transducer. Figure 3 shows an example of the waveforms of the measured voltages and contact displacement curve, where t_{pre} is the instant when the first prestrike occurs and t_{aux} is the instant when the moving contact is mechanically mated to the fixed contact. Finally, the prestrike gap d , i.e., the vacuum gap length between the contacts when the prestrike occurs during the closing operation, can be obtained.

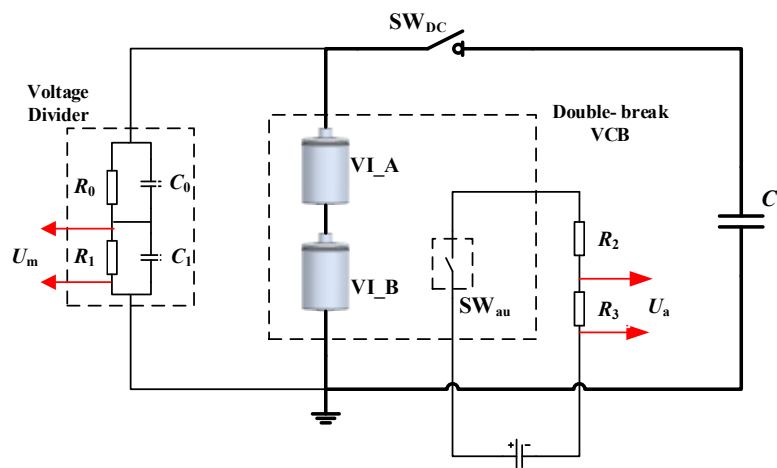


Figure 1. Schematic diagram of the experimental circuit.

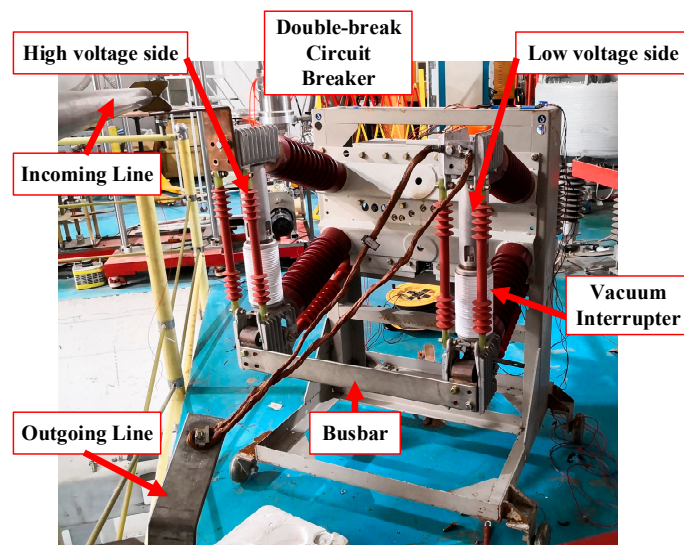


Figure 2. Picture of the experimental setup.

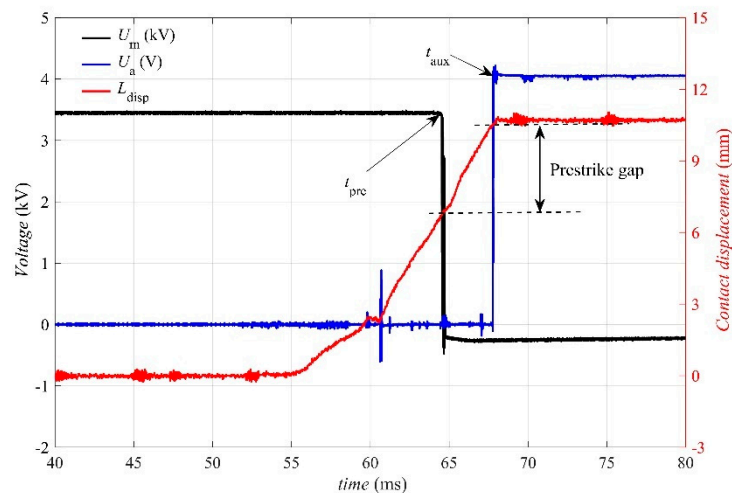


Figure 3. Example of the waveforms of voltages U_m and U_a and the moving.

Three groups of tests were carried out under the experimental conditions that are summarized in Table 1, where the applied DC voltage U_s were set as four levels of 10, 20, 30, 40 kV. In *Test 1* and *Test 2* the prestrike characteristics of vacuum interrupters (VI_A and VI_B) under DC voltages U_s were investigated separately. In this case, only one vacuum interrupter (VI_A or VI_B) was connected into the experimental circuit while the other one was shorted to ground by a busbar. In *Test 3*, the prestrike characteristics of the double-break VCB with two vacuum interrupters (VI_A together with VI_B) in series were analyzed, where VI_A was installed in the high-voltage side of the VCB and VI_B the low-voltage side (Figure 1). In this case, the total prestrike gap d was defined as the sum of the prestrike gaps in VI_A and in VI_B. The current-making operations were repeated 30 times in each test for all the test groups.

Table 1. Experimental conditions.

| Test Group | Applied Voltage (kV) | Experimental Condition | Making Operation |
|---------------|----------------------|--|------------------|
| <i>Test 1</i> | U_s | Single-break test with VI_A | 30 |
| <i>Test 2</i> | U_s | Single-break test with VI_B | 30 |
| <i>Test 3</i> | U_s | Double-break test with VI_A and VI_B in series | 30 |

The prestrike arc current during each current-making operation was only tens to hundreds of amperes. Considering all the contact surfaces had already been well conditioned, the erosion effect on the contact surfaces was low and could be neglected. Moreover, because of the asynchronous property of the mechanical actuators in the double-break VCB, the contacts in VI_A and VI_B were not mechanically closed at the same time. The average time delay of VI_B compared with VI_A was 0.1 ms (computed from 50 closing operations with no load), which was used as a compensation when calculating the time instant t_{aux} .

3. Experimental Results

3.1. Probabilistic Characteristics of the Prestrike Gap

The prestrike phenomenon in the vacuum circuit breakers can be characterized by prestrike gap d , which is the instantaneous vacuum gap length between the contacts of the vacuum interrupters. It is measured at the occurrence of the first prestrike during a current-making operation. In this work, a probabilistic analysis of the prestrike gap under different applied voltage levels had been carried out. The distributions of the prestrike gaps in the test groups under each voltage level were calculated. Let $f(d)$ be the density function (DF) of the prestrike gap distributions, which indicates the chance of the prestrike between the contacts in VIs at a vacuum gap length d . The corresponding complementary cumulative distribution function (CCDF) can be then calculated by:

$$F(d) = \int_d^{\infty} f(u)du \quad (1)$$

which gives the probability of the prestrike between the contacts in VIs when the vacuum gap length is no less than d . Figures 4–6 show the calculated CCDF under applied voltage U_s from the experimentally measured prestrike gaps in *Test 1*, *Test 2* and *Test 3*, respectively. In *Test 3*, the total prestrike gap as well as the prestrike gaps in VI_A (high voltage side) and in VI_B (low voltage side) were all given.

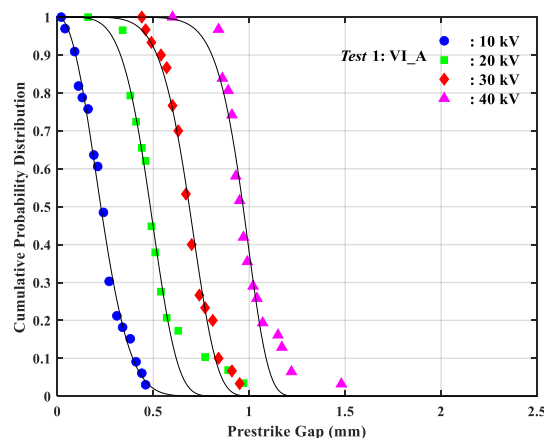


Figure 4. The complementary cumulative distribution function of prestrike gaps in *Test 1*.

For the characterization of the CCDF, the Weibull distribution is used and the CCDF is then given by:

$$F(d) = \exp\left(-\left(\frac{d}{\eta}\right)^\beta\right) \quad (2)$$

where $\eta > 0$ is the shape parameter of the Weibull distribution [24] and $\beta > 0$ is the scale parameter of the Weibull distribution or the characteristic value of the prestrike gap. Both η and β are obtained by fitting the experimental data, as shown in Table 2.

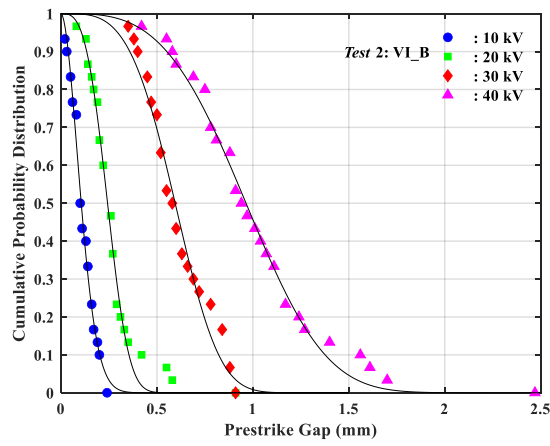
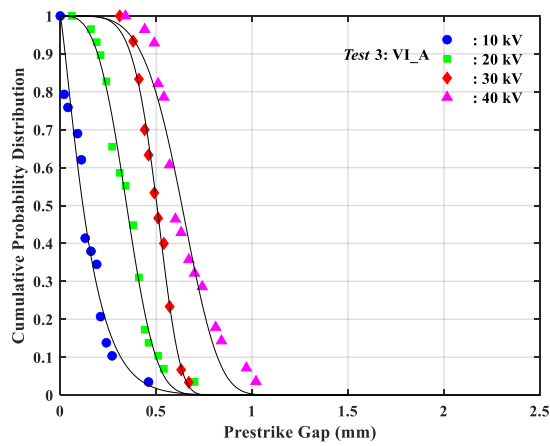
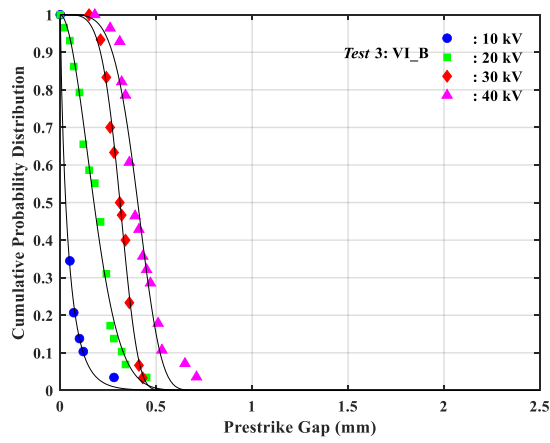


Figure 5. The complementary cumulative distribution function of prestrike gaps in Test 2.



(a)



(b)

Figure 6. Cont.

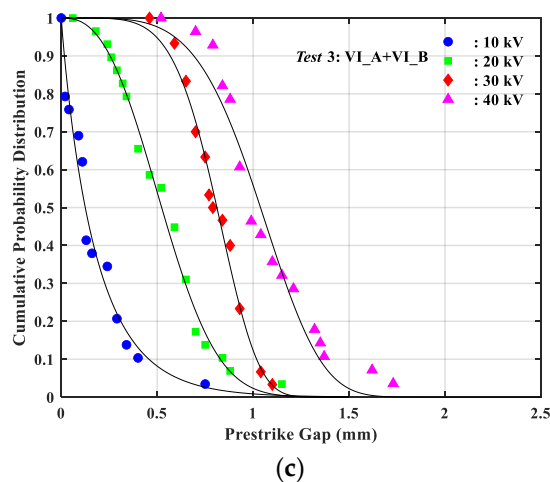


Figure 6. The complementary cumulative distribution function of prestrike gaps in *Test 3* with VI_A and VI_B in series: complementary cumulative distribution function (CCDF) of prestrike gaps in VI_A (a), in VI_B (b), and CCDF of the total prestrike gaps (c).

Table 2. Values of the Weibull parameters.

| Test Group | U_s (kV) | β | η (mm) | R-Square | |
|----------------------|------------|---------|-------------|----------|------|
| <i>Test 1</i> (VI_A) | 10 | 2.2 | 0.3 | 0.99 | |
| | 20 | 4.9 | 0.5 | 0.98 | |
| | 30 | 6.7 | 0.7 | 0.99 | |
| | 40 | 10.3 | 1.0 | 0.95 | |
| <i>Test 2</i> (VI_B) | 10 | 1.8 | 0.1 | 0.99 | |
| | 20 | 3.2 | 0.3 | 0.99 | |
| | 30 | 3.7 | 0.7 | 0.97 | |
| | 40 | 3.4 | 1.1 | 0.99 | |
| VI_A and VI_B | 10 | 0.9 | 0.2 | 0.97 | |
| | 20 | 2.6 | 0.6 | 0.99 | |
| | 30 | 5.3 | 0.9 | 0.99 | |
| | 40 | 4.6 | 1.1 | 0.97 | |
| <i>Test 3</i> | VI_A | 10 | 1.2 | 0.2 | 0.95 |
| | | 20 | 3.3 | 0.4 | 0.99 |
| | | 30 | 5.9 | 0.5 | 0.99 |
| | | 40 | 4.7 | 0.7 | 0.96 |
| VI_B | 10 | 0.8 | 0.04 | 0.99 | |
| | 20 | 1.9 | 0.2 | 0.99 | |
| | 30 | 4.7 | 0.3 | 0.99 | |
| | 40 | 4.7 | 0.4 | 0.97 | |

The fitted curves with the Weibull distribution given in (2) with respect to *Test 1*, *Test 2* and *Test 3* are shown in Figures 4–6, respectively, where a good agreement between the fitted curves and the experimental data can be observed. Besides the evaluation of the fit from the figures graphically, R-square is used in order to evaluate the goodness of the fit numerically, which is the square of the correlation between the predicted prestrike gaps and the experimentally measured values. R-square can take on any value between zero and one, where a value closer to one indicates a better performance of the fitted model [24–26]. The calculated values of the R-square parameter are presented in the last column of Table 2. From Table 2 it can be noted that the values of R-square are no smaller than 95% in all tests, which indicates that the prestrike gap has a Weibull distribution with parameters η and β

and that the model with the given parameters fits the prestrike gap distributions well. CCDF density function $f(d)$ is given by

$$f(d|\eta, \beta) = \frac{\beta}{\eta} \left(\frac{d}{\eta}\right)^{\beta-1} \exp\left(-\left(\frac{d}{\eta}\right)^\beta\right) \quad (3)$$

3.2. Scatters in the Prestrike Gap

The scatter in the prestrike gap is of significant importance for investigating the prestrike phenomenon in vacuum interrupters. Moreover, for the phase-controlled switching application with vacuum circuit breakers, a better knowledge of the scatter in the prestrike gap could help to improve control accuracy. The scatter in the prestrike gap can be characterized by the standard deviation of the experimental measurement of the prestrike gaps, which is given by:

$$\sigma = \sqrt{\frac{1}{N} \sum_{i=1}^N (d_i - \bar{d})^2} \quad (4)$$

where N is the number of each experimental data set; \bar{d} is the average value of each set of the experimental data, and d_i is the prestrike gap measured during the i_{th} making operation. The scatters in the prestrike gaps in all the test groups under varied applied voltages are given in Table 3. In the last column, σ indicates the scatter, where a larger value of σ indicates more scatter in the experimental data of the prestrike gaps.

Table 3. Prestrike gaps of 10%, 50% and 90% and scatters in prestrike gaps.

| Test Group | U_s (kV) | d_{10} (mm) | d_{50} (mm) | d_{90} (mm) | σ (mm) | |
|---------------|------------|---------------|---------------|---------------|---------------|------|
| Test 1 (VI_A) | 10 | 0.39 | 0.23 | 0.10 | 0.11 | |
| | 20 | 0.62 | 0.48 | 0.33 | 0.16 | |
| | 30 | 0.82 | 0.69 | 0.52 | 0.12 | |
| | 40 | 1.09 | 0.97 | 0.81 | 0.15 | |
| Test 2 (VI_B) | 10 | 0.20 | 0.11 | 0.04 | 0.06 | |
| | 20 | 0.35 | 0.24 | 0.13 | 0.16 | |
| | 30 | 0.82 | 0.60 | 0.36 | 0.17 | |
| | 40 | 1.38 | 0.96 | 0.55 | 0.41 | |
| VI_A and VI_B | 10 | 0.46 | 0.13 | 0.02 | 0.16 | |
| | 20 | 0.83 | 0.52 | 0.25 | 0.23 | |
| | 30 | 1.02 | 0.81 | 0.57 | 0.16 | |
| | 40 | 1.35 | 1.04 | 0.69 | 0.27 | |
| Test 3 | VI_A | 10 | 0.32 | 0.12 | 0.03 | 0.11 |
| | | 20 | 0.50 | 0.35 | 0.19 | 0.13 |
| | | 30 | 0.62 | 0.50 | 0.37 | 0.09 |
| | | 40 | 0.82 | 0.63 | 0.42 | 0.16 |
| VI_B | 10 | 0.12 | 0.03 | 0.00 | 0.06 | |
| | 20 | 0.33 | 0.18 | 0.07 | 0.10 | |
| | 30 | 0.40 | 0.31 | 0.21 | 0.07 | |
| | 40 | 0.52 | 0.40 | 0.27 | 0.11 | |

To study the probabilistic characteristics of prestrike gaps, the 10% prestrike gap d_{10} , 50% prestrike gap d_{50} , and 90% prestrike gap d_{90} , i.e., the prestrike gap at which the value of CCDF is 10%, 50%, and 90%, respectively, are commonly used [7,16,25,26]. In this case, the influence of the approximation error between the fitted CCDF and the measured prestrike gaps that are higher than d_{90} or lower than d_{10} on the probabilistic characteristics of prestrike gaps can be neglected. The values of d_{10} , d_{50} , and d_{90} can be calculated by (2), which are shown in Table 3. It can be noted that with the increment of applied voltage U_s , the d_{10} , d_{50} and d_{90} are all increasing significantly. Moreover, the 50% prestrike gap d_{50} can

be used as one of the most important parameters since it gives the prestrike gap at which there is a 50% chance for the vacuum gap to achieve breakdown in the VCB, i.e., d_{50} acts as the mean value of the prestrike gap in the sense of the Weibull distribution. The relationships between d_{50} and applied voltage U_s in *Test 1*, *Test 2*, and *Test 3* are shown in Figure 7, Figure 8, and Figure 9, respectively, where the error bar at each data point shows the corresponding scatter in the prestrike gaps. It can be noted that the value of d_{50} is approximately proportional to applied voltage U_s .

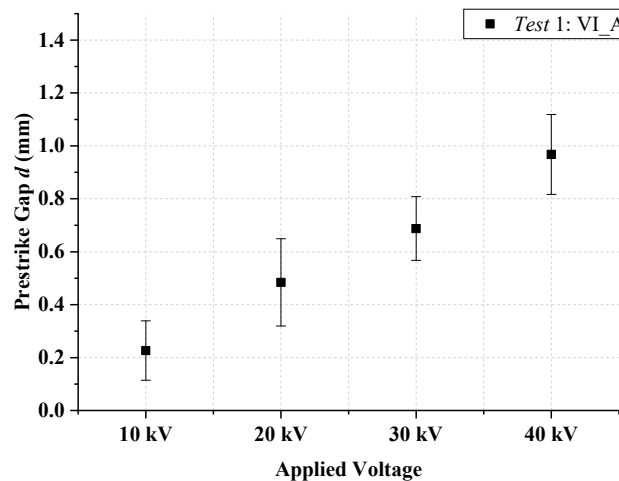


Figure 7. The relationships between d_{50} and applied voltage U_s in *Test 1* with VI_A.

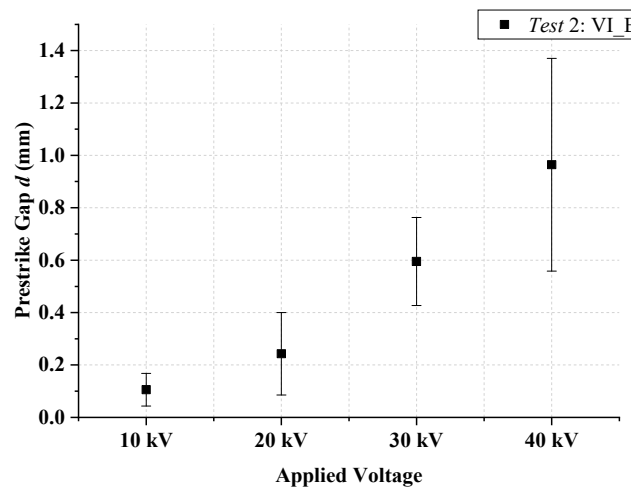
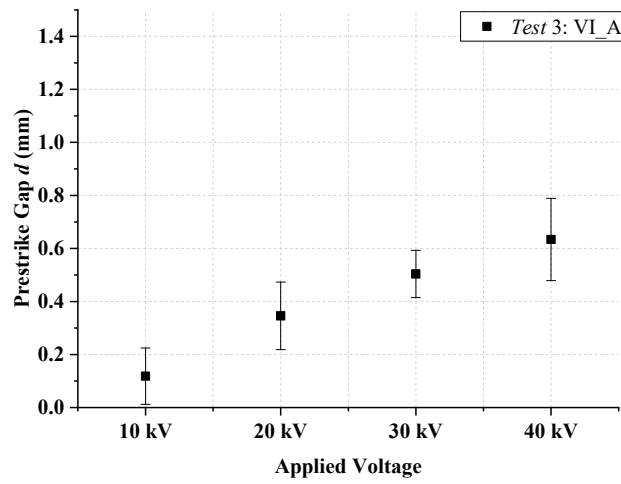
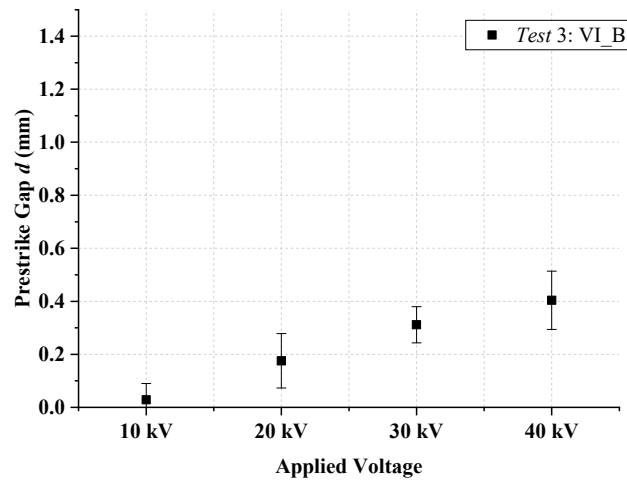


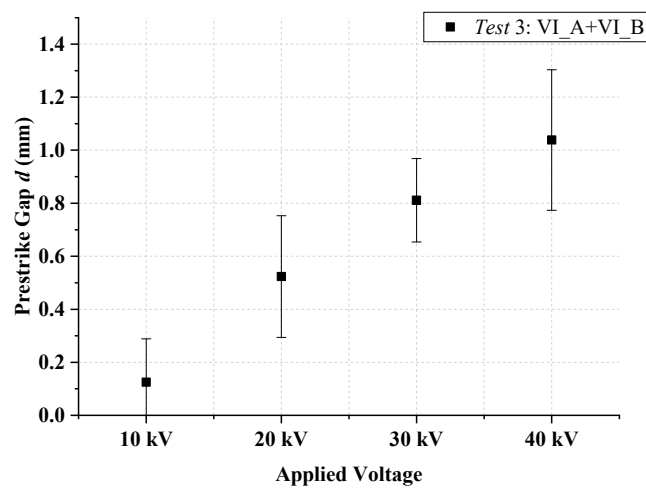
Figure 8. The relationships between d_{50} and applied voltage U_s in *Test 2* with VI_B.



(a)



(b)



(c)

Figure 9. The relationships between d_{50} and applied voltage U_s in Test 3: VI_A (a), VI_B (b), and the total prestrike gaps (c).

4. Discussion

4.1. Positive Effects of the Double-Break Vacuum Circuit Breaker

A vacuum interrupter in the double-break tests (*Test 3*) may have different prestrike characteristics in terms of prestrike gaps and scatters in prestrike gaps compared with that in the single-break tests (*Test 1* and *Test 2*) due to the voltage-sharing-effect, the asynchronous property of the mechanical actuators, and the inhomogeneity of the inherent prestrike characteristics of VIs in a double-break VCB.

From Table 3, it can be noted that the scatters in the prestrike gaps of VI_A (resp., VI_B) in the double-break tests, i.e., in *Test 3* are smaller than that of VI_A (VI_B) in the single-break tests, i.e., in *Test 1* (with respect to *Test 2*). Vacuum interrupters with less scatters in the prestrike gaps would be of great importance in order to improve the accuracy of the phase-controlled making technique. Therefore, with the same VIs, a double-break VCB would be better suitable for the phase-controlled switching.

The double-break VCB takes full advantage of the good dielectric insulation ability of the vacuum gap. A double-break VCB which has two gaps in series can withstand higher voltage compared to the single-break VCB in the same total break length [27]. The relationship between breakdown voltage and electrodes gap of the single-break VCB has two different expressions. When the electrode gap is less than 5 mm, the breakdown voltage and electrodes gap length is a linear equation, as shown in:

$$U_t = k \cdot d \quad (5)$$

When the electrode gap is greater than 5 mm, Breakdown voltage and electrodes gap length is a non-linear equation when the electrodes' distance is greater than 5 mm, as shown in:

$$U_t = k \cdot d^m \quad (6)$$

The value of m is between 0.4 to 0.7, d stands for the electrodes' gap length, k is a constant number.

The relationship between breakdown voltage and electrodes' gap length of the double-break VCB is shown in (7). It is based on the assumption that the voltage distribution value of two interrupters is equal.

$$U_t = 2k \cdot d^m \quad (7)$$

However, in the double-break VCB which does not have a grading capacitor in parallel with each VI, the shared voltages of each VI are not equal because of the stray capacitance. It is impossible to realize double withstand voltage as (7) shows [28]. In order to investigate the influence of the voltage-sharing effect in double-break VCBs on the prestrike characteristics, the relative variations in the prestrike gaps of each vacuum interrupter under different applied voltage levels are calculated by:

$$\delta(d) = \frac{d^{(DB)} - d^{(SB)}}{d^{(SB)}} \times 100\% \quad (8)$$

where $d^{(DB)}$ is the prestrike gap of vacuum interrupter VI_A (resp., VI_B) obtained from the double-break test, i.e., *Test 3* and $d^{(SB)}$ is the prestrike gap from the single-break test, i.e., *Test 1* (resp., *Test 2*).

Table 4 shows the values of relative variations δ in d_{10} , d_{50} and d_{90} . The vacuum gaps in VI_A and VI_B in the double-break test can be considered as two capacitors in series [29] and each gap shared part of the total applied voltage U_s . Therefore, the voltage applied to each gap was smaller than U_s , leading to a smaller prestrike gap. The smaller the prestrike gap was, the shorter the prestrike arcing time was. For a given applied voltage, a double-break VCB has a better performance than a single-break one in terms of reducing the prestrike gaps in the vacuum interrupter, which is termed as the positive effects of double-break VCBs.

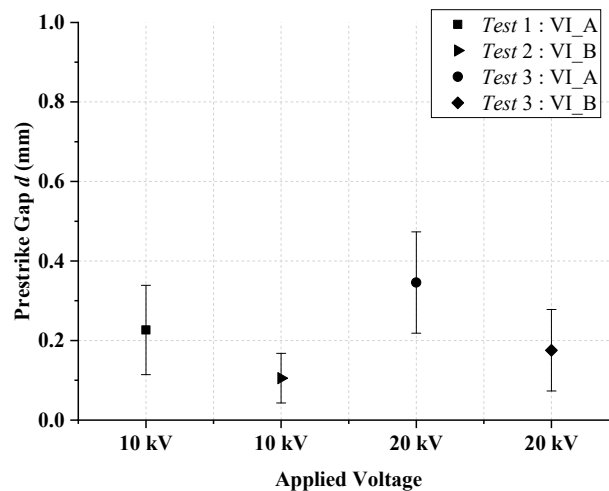
Table 4. Relative variations in the 10%, 50% and 90% prestrike gaps.

| U_s (kV) | | 10 | 20 | 30 | 40 |
|------------|-------------------|--------|--------|--------|--------|
| VI_A | $\delta (d_{10})$ | -17.9% | -19.4% | -24.4% | -24.8% |
| | $\delta (d_{50})$ | -47.8% | -27.1% | -27.5% | -35.1% |
| | $\delta (d_{90})$ | -70% | -42.4% | -28.8% | -48.1% |
| VI_B | $\delta (d_{10})$ | -40% | -5.7% | -51.2% | -62.3% |
| | $\delta (d_{50})$ | -72.7% | -25.0% | -48.3% | -58.3% |
| | $\delta (d_{90})$ | -100% | -46.2% | -41.7% | -50.9% |

4.2. Negative Effects of the Double-Break Vacuum Circuit Breaker

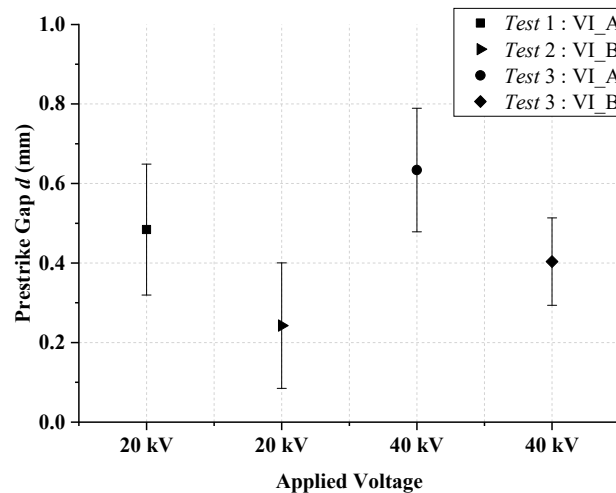
Due to the voltage-sharing effect, the actual voltage applied to each vacuum interrupter VI_A or VI_B in the double-break tests was smaller than that in the single-break tests. In order to investigate the prestrike characteristics of vacuum interrupters in double-break tests by comparison with that in single-break tests under the same applied voltage, the influence of the voltage-sharing effect has to be eliminated.

In an ideal case, if both interrupters VI_A and VI_B share the same percentile of the total applied voltage U_s , i.e., both share 50% out of U_s , then the sharing voltage of VI_A (resp., VI_B) in *Test 3* would be 10 kV or 20 kV, i.e., the same voltage applied to VI_A (resp., VI_B) in *Test 1* (resp., *Test 2*), when the applied voltage to the double-break U_s in *Test 3* is 20 kV or 40 kV. Figure 10 shows the 50% prestrike gap d_{50} of VI_A and VI_B in the single-break tests compared with that in the double-break tests where the value of applied voltage U_s in *Test 3* is twice as large as that in single-break tests (*Test 1* and *Test 2*).



(a)

Figure 10. Cont.



(b)

Figure 10. The negative effects of double-break vacuum circuit breakers (VCBs) on the prestrike gaps of vacuum interrupters. (a) The single-break VCB under 10 kV compared with the double-break under 20kV. (b) The single-break VCB under 20 kV compared with the double-break under 40kV.

However, the voltage-sharing ratio of VI_A and VI_B in double-break VCBs was not the same due to the stray capacitance to ground. In fact, from the previous studies the voltage-sharing ratio of the vacuum interrupter installed on the high voltage side (i.e., VI_A in our case) is larger than that on the low voltage side (VI_B) [30]. Note that a larger applied voltage leads to a higher prestrike gap. Therefore, the prestrike gaps of VI_A in *Test 3* should be larger than that in *Test 1*, while the prestrike gaps of VI_B in *Test 3* should be smaller than that in *Test 2* when U_s in *Test 3* is twice as large as that in *Test 1* and *Test 2*. This can be verified for the vacuum interrupter VI_A from Figure 10, but not for VI_B. As can be observed from Figure 10, the prestrike gap of VI_B in *Test 3* is larger. To be precise, the voltage applied to VI_B in *Test 3* with $U_s = 20$ kV (resp., 40 kV) is lower than 10 kV (resp., 20 kV) due to the voltage-sharing effect while the 50% prestrike gaps d_{50} is larger than that in *Test 2* with an applied voltage of 10 kV (with respect to 20 kV) instead. That is to say, the double-break VCB does not make fully advantage of the dielectric strength of the vacuum gap on the low voltage side, which is termed as the negative effects of double-break VCBs.

The negative effects of double-break VCBs may be caused by the asynchronous property of the mechanical actuators, the inhomogeneity of the inherent prestrike characteristics and the unequal voltage-sharing ratio of VIs in a double-break VCB.

The double-break VCB is closed or interrupted by the mechanical actuators. In the ideal case, the two VIs of the double-break VCB moves at the same velocity and the operating characteristics are same too. Due to the inevitable performance differences between the mechanism's actuators of the double-break VCB, and their tolerance to various environmental changes not being the same, the effect caused by the asynchronous property of the mechanical actuators on the double-break VCB must not be underestimated. In the breaking process, when the operating time interval of two breaks is 2 ms, the distance difference between two vacuum gaps is significant. The arcing time of the two VIs is different, which makes the sharing voltage of each VI is unequal in the breaking process. In the most serious situation, reignition will occur [31]. On the other hand, in the current-making process, considering a double-break VCB with two vacuum interrupters VI_A and VI_B in series, we denote by $d_{50}^*(VI_A)$ and $d_{50}^*(VI_B)$ the inherent 50% prestrike gaps of VI_A and VI_B, which is the 50% prestrike gap when tested separately in the single-break tests. Due to the asynchronous property of the mechanical actuators in the double-break VCB, one of the moving contacts, for example the moving contact in VI_A, moves faster than the other, as shown in Figure 11a. Let both VI_A and VI_B share half of the applied voltage ($U_s/2$) and have a same inherent 50% prestrike gap, i.e., $d_{50}^*(VI_A) = d_{50}^*(VI_B)$.

During the closing operation, the vacuum gap length between the contacts in VI_A is smaller than that in VI_B ($l_A < l_B$). Therefore, it is very possible for VI_A to breakdown earlier than VI_B. As soon as the prestrike occurs in VI_A, the total voltage U_s would be applied to the vacuum gap in VI_B. Then the prestrike occurs in VI_B. In this case, the measured prestrike gap of VI_B is the same as l_A , which is larger than $d_{50}^*(VI_B)$ the inherent 50% prestrike gap of VI_B.

Moreover, let both VI_A and VI_B be synchronized perfectly and share half of the applied voltage ($U_s/2$), as shown in Figure 11b. The inherent 50% prestrike gap of VI_A is larger than that of VI_B, i.e., $d_{50}^*(VI_A) > d_{50}^*(VI_B)$. Then, it is very possible that the prestrike occurs in VI_A earlier than in VI_B, leading to a higher prestrike gap of VI_B (that is l_B) than $d_{50}^*(VI_B)$.

Similar effects can also be found in the case when the voltage-sharing ratios of VI_A and VI_B are not equal to each other. As shown in Figure 11c, both VI_A and VI_B are synchronized perfectly and have the same inherent 50% prestrike gap, since VI_A on the high voltage side shares voltage higher than $U_s/2$. The interrupter VI_A is highly possible to breakdown when the vacuum gap length is larger than the inherent 50% prestrike gap, i.e., $l_A > d_{50}^*(VI_A)$. Noting VI_A and VI_B are perfectly synchronized ($l_A = l_B$), the measured 50% prestrike gap of VI_B would be larger than its inherent one.

The mechanical actuators of the double-break VCB used in this work are not perfectly synchronized, which is practically impossible. The mechanical actuator installed on the low-voltage side moves slower than that on the high voltage side with a time delay of 0.1 ms. Moreover, from Table 3, the inherent 50% prestrike gap of VI_A is always larger than that of VI_B under the tested applied voltages. Together with the effect of the unequal voltage-sharing ratio, the negative effects of double-break VCBs are observed as shown in Figure 10.

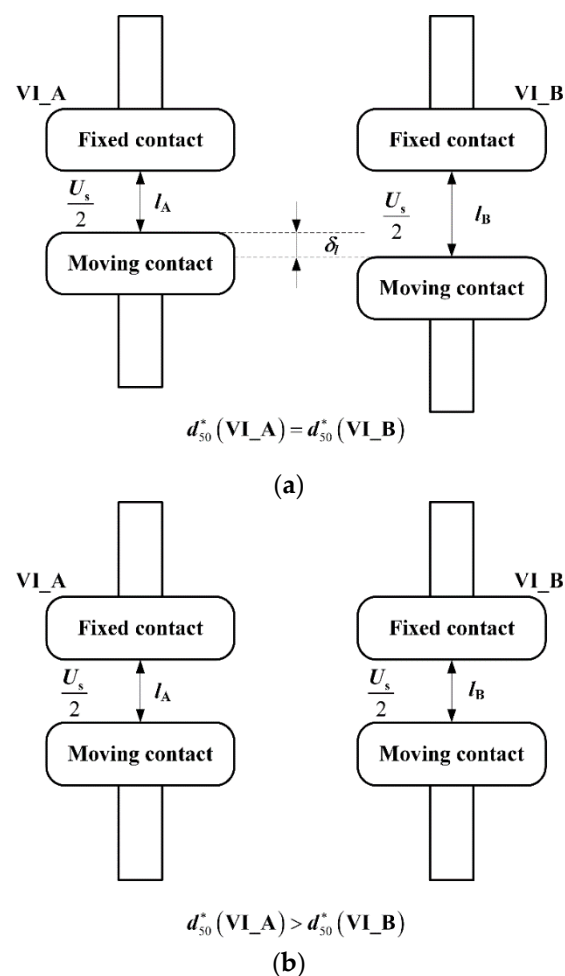


Figure 11. Cont.

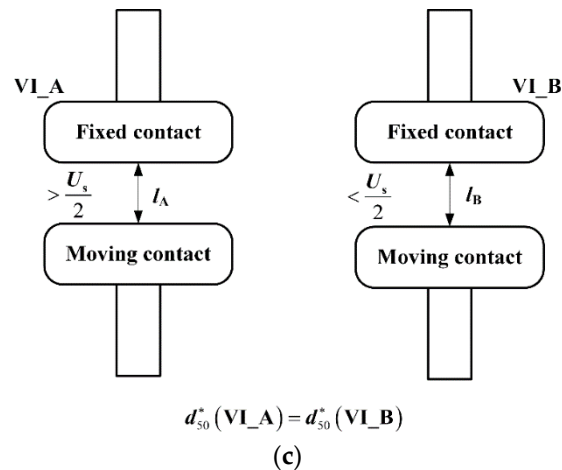


Figure 11. Schematic diagram of the negative effects of the double-break VCBs in terms of the asynchronous property of the mechanical actuators (a), the inhomogeneity of the inherent prestrike gaps (b), and the unequal voltage-sharing ratio (c).

The prestriking phenomena are irrelevant to the initial contact gaps in the double break and the single break in this work. As for the experimental setup, the double-break VCB consisted of two VIs. When carrying out the single-break tests, only one vacuum interrupter (VI_A or VI_B) was connected into the experimental circuit while the other one was shorted to ground by the busbar. The initial gaps of both VIs were 10 mm. Therefore, the initial gap of the single-break VCBs was 10 mm, and the initial gap of the double-break VCB was 20 mm (two 10 mm gaps in series). There are mainly two theories about the breakdown in the vacuum. One is that field emission induces breakdown, the other is that particles induce vacuum breakdown [6]. If the vacuum gap is less than 2 mm, the field emission plays the dominant role in the breakdown process [9]. In these tests, all the prestrike gaps were less than 2 mm. The prestrike was field-emission induced. The prestrike arc current during each making operation was only tens to hundreds of amperes, the erosion effect on the contact surfaces can be neglected. During the making process of the VCB, there is a threshold electric field strength that determined whether breakdown occurs or not [32]. When the electric field strength exceeds the threshold electric field strength between the contacts, the prestrike arc occurs and the gap between the contacts at that instant is called prestrike gap, which is independent of the initial gap of the VCB [33]. However, if there is an inrush current in the prestrike process that causes erosion on contacts or the prestrike gaps are larger than 2 mm, the initial gap of the single-break VCB and the double-break VCB must be kept the same in order to compare the characteristics of prestrike gaps.

5. Conclusions

In this paper, the prestrike characteristics of a double-break VCB consisting of two 12 kV VIs in series under DC voltages had been experimentally analyzed. The following conclusions can be drawn.

- (1) With the increment of the applied DC voltage, the 10% prestrike gap d_{10} , 50% prestrike gap d_{50} and 90% prestrike gap d_{90} were all increasing significantly, whereas the scatters in the prestrike gaps were not changing too much. Specifically, the value of d_{50} was approximately proportional to the applied voltage.
- (2) With a given applied DC voltage, the positive effect of the double-break VCBs on the prestrike characteristics can be observed, i.e., the prestrike gaps of the vacuum interrupters in the double-break tests can be significantly reduced in comparison with that in the single-break tests due to the voltage-sharing effect in double-break VCBs. Moreover, fewer scatters in the prestrike gaps during the double-break tests can be found.
- (3) The double-break VCB with two vacuum interrupters in series did not take full advantage of the dielectric strength of the vacuum gap on the low-voltage side, i.e., the negative effect of a

double-break VCB on the prestrike characteristics, which may be caused by the asynchronous property of the mechanical actuators, the inhomogeneity of the inherent prestrike characteristics and the unequal voltage-sharing ratio of VIs in a double-break VCB.

Author Contributions: Y.G. (Yun Geng) and X.Y. contributed to the research idea and designed the experiments. Y.G. (Yun Geng) and J.D. worked on the data analysis and drafted the manuscript. X.L. and J.P. helped to do the experiments. Y.G. (Yingsan Geng), Z.L. and K.W. worked on editing and revising of the manuscript. All authors have read and approved the final manuscript.

Funding: This work was supported in part by the National Natural Science Foundation of China under Grant 51937009, Key Research and Development Program of Shaanxi (2019ZDLGY18-04), the Fundamental Research Funds for the Central Universities (xzy022019013).

Conflicts of Interest: The authors declare no conflict of interest.

References

- Ide, N.; Tanaka, O.; Yanabu, S.; Kaneko, S.; Okabe, S.; Matsui, Y. Interruption characteristics of double-break vacuum circuit breakers. *IEEE Trans. Dielectr. Electr. Insul.* **2008**, *15*, 1065–1072. [[CrossRef](#)]
- Ge, G.; Liao, M.; Duan, X.; Cheng, X.; Zhao, Y.; Liu, Z.; Zou, J. Experimental Investigation into the Synergy of Vacuum Circuit Breaker with Double-Break. *IEEE Trans. Plasma Sci.* **2016**, *44*, 79–84. [[CrossRef](#)]
- Giere, S.; Karner, H.C.; Knobloch, H. Dielectric strength of double and single-break vacuum interrupters: Experiments with real HV demonstration bottles. *IEEE Trans. Dielectr. Electr. Insul.* **2001**, *8*, 43–47. [[CrossRef](#)]
- Fugel, T.; Koenig, D. Switching performance of two 24 kV vacuum interrupters in series. *IEEE Trans. Dielectr. Electr. Insul.* **2002**, *9*, 164–168. [[CrossRef](#)]
- Delachaux, T.; Rager, F.; Gentsch, D. Study of vacuum circuit breaker performance and weld formation for different drive closing speeds for switching capacitive current. In Proceedings of the 24th International Symposium on Discharges and Electrical Insulation in Vacuum (ISDEIV2010), Braunschweig, Germany, 30 August–3 September 2010; pp. 241–244.
- Zhang, Y.; Xu, X.; Jin, L.; An, Z.; Zhang, Y. Fractal-based electric field enhancement modeling of vacuum gap electrodes. *IEEE Trans. Dielectr. Electr. Insul.* **2017**, *24*, 1957–1964. [[CrossRef](#)]
- Slade, P.G. *The Vacuum Interrupter Theory, Design and Application*; CRC Press: Boca Raton, FL, USA, 2008.
- Descoedres, A.; Ramsvik, T.; Calatroni, S.; Taborelli, M.; Wuensch, W. DC breakdown conditioning and breakdown rate of metals and metallic alloys under ultrahigh vacuum. *Phys. Rev. Spec. Top. Accel. Beams* **2009**, *12*. [[CrossRef](#)]
- Latham, R.V. *High Voltage and Vacuum Insulation: Basic Concepts and Technological Practice*; Academic Press: London, UK, 1995.
- Slade, P.G.; Taylor, E.D.; Haskins, R.E. Effect of short circuit current duration on the welding of closed contacts in vacuum. In Proceedings of the 51th IEEE Holm Conference on Electrical Contacts, Chicago, IL, USA, 26–28 September 2005; pp. 69–74.
- Slade, P.G.; Smith, R.K.; Taylor, E.D. The effect of contact closure in vacuum with fault current on prestrike arcing time, contact welding and the field enhancement factor. In Proceedings of the 2007 53rd IEEE Holm Conference on Electrical Contacts, Pittsburgh, PA, USA, 16–19 September 2007; pp. 32–36.
- Dullni, E.; Shang, W.; Gentsch, D.; Kleberg, I.; Niayesh, K. Switching of Capacitive Currents and the Correlation of Restrike and Pre-ignition Behavior. *IEEE Trans. Dielectr. Electr. Insul.* **2006**, *13*, 65–71. [[CrossRef](#)]
- Körner, F.; Lindmayer, M.; Kurrat, M.; Gentsch, D. Contact Behavior in vacuum under capacitive switching duty. *IEEE Trans. Dielectr. Electr. Insul.* **2007**, *14*, 643–648. [[CrossRef](#)]
- Körner, F.; Lindmayer, M.; Kurrat, M.; Gentsch, D. Switching behavior of different contacts materials under capacitive switching conditions. In Proceedings of the 23rd International Symposium on Discharges Electrical Insulation in Vacuum, Braunschweig, Germany, 15–19 September 2008; pp. 202–205.
- Kumichev, G.A.; Poluyanova, I.N. Investigation of welding characteristics and NSDD probabilities of different contact materials under capacitive load conditions. In Proceedings of the 27th International Symposium on Discharges and Electrical Insulation in Vacuum (ISDEIV), Suzhou, China, 18–23 September 2016; pp. 1–4.

16. Yu, Y.; Li, G.; Geng, Y.; Wang, J.; Liu, Z. Prestrike inrush current arc behaviors in vacuum interrupters subjected to a transverse magnetic field and an axial magnetic field. *IEEE Trans. Plasma Sci.* **2018**, *46*, 3075–3082. [[CrossRef](#)]
17. Yu, Y.; Geng, Y.; Geng, Y.; Wang, J.; Liu, Z. Inrush current prestrike arc behaviours of contact materials CuCr50/50 and CuW10/90. *IEEE Trans. Plasma Sci.* **2017**, *45*, 266–274. [[CrossRef](#)]
18. Geng, Y.; Yu, Y.; Geng, Y.; Wang, J.; Liu, Z. Inrush current arc characteristics in vacuum interrupters with axial magnetic field contact and butt-type contact. In Proceedings of the 3rd International Conference on Electric Power Equipment—Switching Technology (ICEPE-ST2015), Busan, Korea, 25–28 October 2015; pp. 512–515.
19. Razi-Kazemi, A.A.; Fallah, M.R.; Rostami, M.; Malekipour, F. A new realistic transient model for restriking/prestrike phenomena in vacuum circuit breaker. *Int. J. Electr. Power Energy Syst.* **2020**, *117*. [[CrossRef](#)]
20. Ma, X.; McLester, M.; Sudarshan, T.S. Prebreakdown and breakdown characteristics of micrometric vacuum gaps between broad area electrodes. In Proceedings of the IEEE 1997 Annual Report Conference on Electrical Insulation and Dielectric Phenomena, Minneapolis, MN, USA, 19–22 October 1997; pp. 583–586.
21. Kharin, S.N.; Nouri, H.; Amft, D. Dynamics of electrical contact floating in vacuum. In Proceedings of the 48th IEEE Holm Conference on Electrical Contacts, Orlando, FL, USA, 22–23 October 2002; pp. 197–205.
22. Kharin, S.N.; Ghori, Q.K. Influence of the pre-arcing bridging on the duration of vacuum arc. In Proceedings of the 19th International Symposium on Discharges and Electrical Insulation in Vacuum, Xi'an, China, 18–22 September 2000; pp. 278–285.
23. Sima, W.; Zou, M.; Yang, Q.; Yang, M.; Li, L. Field experiments on 10 kV switching shunt capacitor banks using ordinary and phase-controlled vacuum circuit breakers. *Energies* **2016**, *9*, 88. [[CrossRef](#)]
24. Mccool, J.I. *Using the Weibull Distribution Reliability: Modeling, and Inference*; Wiley & Sons Inc.: Hoboken, NJ, USA, 2012.
25. Zhang, Y.; Yang, H.; Wang, J.; Geng, Y.; Liu, Z.; Jin, L.; Yu, L. Influence of high-frequency high-voltage impulse conditioning on back-to-back capacitor bank switching performance of vacuum interrupters. *IEEE Trans. Plasma Sci.* **2016**, *44*, 321–330. [[CrossRef](#)]
26. Yang, H.; Geng, Y.; Liu, Z.; Zhang, Y.; Wang, J. Capacitive switching of vacuum interrupters and inrush currents. *IEEE Trans. Dielectr. Electr. Insul.* **2014**, *21*, 159–170. [[CrossRef](#)]
27. Cheng, X.; Liao, M.; Duan, X.; Zou, J. Experimental research on dynamic dielectric recovery characteristics for vacuum switch with double-break. In Proceedings of the 2011 IEEE Pulsed Power Conference, Chicago, IL, USA, 19–23 June 2011; pp. 291–296.
28. Shiba, Y.; Ide, N.; Ichikawa, H.; Matsui, Y.; Sakaki, M.; Yanabu, S. Withstand Voltage Characteristics of Two Series Vacuum Interrupters. *IEEE Trans. Plasma Sci.* **2007**, *35*, 879–884. [[CrossRef](#)]
29. Liao, M.; Duan, X.; Cheng, X.; Zou, J. Dynamic dielectric recovery property for vacuum circuit-breakers with double breaks. In Proceedings of the 24th International Symposium on Discharges and Electrical Insulation in Vacuum (ISDEIV2010), Braunschweig, Germany, 30 August–3 September 2010; pp. 225–228.
30. Fugel, T.; Koenig, D. Breaking performance of a capacitive-graded series design of two 24-kV vacuum circuit breakers. In Proceedings of the 20th International Symposium on Discharges and Electrical Insulation in Vacuum (ISDEIV2002), Tours, France, 1–5 July 2002; pp. 360–363.
31. Betz, T.; Konig, D. Influence of grading capacitors on the breaking capacity of two vacuum interrupters in series. *IEEE Trans. Dielectr. Electr. Insul.* **1999**, *6*, 405–409. [[CrossRef](#)]
32. Li, S.; Geng, Y.; Liu, Z.; Wang, J. A breakdown mechanism transition with increasing vacuum gaps. *IEEE Trans. Dielectr. Electr. Insul.* **2017**, *24*, 3340–3346.
33. Wei, L.; Chun-En, F.; Bi-De, Z.; Pian, X.; Xiao, R.; Yan, L. Research on controlled switching in reducing unloaded power transformer inrush current considering circuit breaker's prestrike characteristics. In Proceedings of the 27th International Symposium on Discharges and Electrical Insulation in Vacuum (ISDEIV 2016), Suzhou, China, 18–23 September 2016; pp. 1–4.

